Journal of
Ceramic Science
and Technology

J. Ceram. Sci. Tech., **08** [01] 101-112 (2017)
DOI: 10.4416/JCST2016-00094
available online at: http://www.ceramic-science.com

Reaction Heat Utilization in Aluminosilicate-Based Ceramics Synthesis and Sintering

M. Karhu*[1], J. Lagerbom[1], P. Kivikytö-Reponen[1], A. Ismailov[2], E. Levänen[2]

[1]VTT Technical Research Centre of Finland Ltd, Sinitaival 6, P.O. Box 1300, FI-33101 Tampere, Finland
[2]Tampere University of Technology, Korkeakoulunkatu 10, P.O. Box 527, FI-33101 Tampere, Finland

received November 2, 2016; received in revised form December 16, 2016; accepted January 19, 2017

Abstract

Self-propagating high-temperature synthesis (SHS) is a widely known and extensively studied highly exothermic-reaction-utilizing technique for making certain advanced composites and intermetallic compounds. However, only few studies have been published about the SHS of pure aluminosilicate ceramics. In the current work, possibilities for aluminosilicate ceramic synthesis and sintering requiring less energy based on the utilization of SHS in air was studied. Kaolinite powder and exothermically reactive metallic aluminium powder were used as raw materials. Thermodynamic calculations for the possible reactions and reaction paths were performed to show the theoretical possibilities for SHS utilization. The chemical reactions, thermal expansion behaviour and formed phase- and microstructures after SHS were compared to the conventional reaction sintering of mullite. Results conclude that highly exothermic reactions above 900 °C relating mainly to aluminium oxidation can ignite the SHS reaction in air atmosphere. After initialization, the reaction proceeded in a self-sustaining manner through entire test pieces, resulting in the formation of an Al_2O_3 - Si phase structure. Thermodynamic calculations showed the total energy balance for mullite formation from aluminium and kaolinite mixtures as highly exothermic in nature only if sufficient oxygen is available to complete the reactions. However, future research is needed to fully utilize SHS in aluminosilicate ceramics processing.

Keywords: Aluminosilicate ceramics, self-propagating high-temperature synthesis, SHS, exothermic reactions, synthesis, sintering

I. Introduction

Ceramics processing, e.g. mullite reaction sintering, normally requires high temperatures and long processing times that consume a lot of energy, increasing the cost of the products and leading to a high environmental impact. One process technology opportunity to lower processing energy is to utilize the reaction heat released from exothermic ceramic compound reactions. A lower overall energy consumption can then be achieved by producing part of the heat internally in the process and utilizing this extra heat in ceramic material processing and synthesis. One widely known and extensively studied technique utilizing highly exothermic reactions is self-propagating high temperature synthesis (SHS). SHS is based on a system's ability to react exothermally and proceed when ignited. The high activation energy and high compound formation enthalpy of the synthesis reaction is utilized to run a self-sustained reaction; thus, once ignited, the reaction continues on its own [1,2]. When the initial reagents are ignited, they spontaneously transform into products and a reaction front is formed that propagates through the reactants in the form of a combustion wave. Owing to the exothermic heat of reaction and subsequent high temperature of the reaction products, it is possible to combine the synthesis and densification steps into one process. The SHS process is traditionally limited only to highly exothermic reactions for making certain advanced composites and intermetallic compounds [3,4].

Mullite is one example of an advanced aluminosilicate ceramic material for high-temperature applications owing to its favourable properties such as high melting point (1830 °C), moderate thermal expansion coefficient (4.5×10^{-6} 1/K), good resistance to thermal shock, good chemical durability, excellent creep resistance and sufficient mechanical strength [5,6]. The stoichiometric 3:2 mullite ($3Al_2O_3$ $2SiO_2$) is the only thermodynamically stable phase in the $SiO_2 \pm Al_2O_3$ system [7]. Various starting materials and preparation methods have been used to prepare mullite ceramics. For the conventional fabrication method, the solid-state reaction of high-purity Al_2O_3 and SiO_2 (quartz), the mullitization temperature is as high as 1600 °C [8]. Kaolinite powder is commonly used as a raw material for mullite synthesis owing to its low cost, and upon heating it reacts to form mullite and silica [9]. There are several studies on mullite reaction sintering, for example in the study by Chen *et al.* [7], it was demonstrated that mullite specimens can be prepared by reaction sintering of mechanically mixed kaolinite and alumina powders.

Few studies have been published about the SHS synthesis of mullite-based composites: zirconia-mullite/TiB_2 composite [6], mullite/TiB_2 composite [8] and TaB/TaB_2/mullite composites [10]. However, only few studies have been pub-

* Corresponding author: marjaana.karhu@vtt.fi

lished about exothermic-assisted synthesis and sintering of pure aluminosilicate-based ceramics. In the recent study by Esharghawi *et al.* [11], porous mullite-based bodies were produced in flowing oxygen by means of SHS starting from kaolin, Al and Mg powder mixtures. They found out that the heat of the aluminium oxidation reaction in a pure oxygen atmosphere could be used to ignite the SHS reaction. A sufficient amount of oxygen was not obtained using air. Pure mullite was not obtained, but in addition to mullite, Si and Al in metallic phases, quartz, α-alumina and $MgAl_2O_4$ spinel were also present after SHS. In the work by Podbolotov *et al.* [12], preparation of aluminosilicate coatings with a mullite weight content of 61 – 72 % by means of SHS was studied using aluminium powder, quartz sand and kaolinite clay as raw materials together with different binders and additives. The exact compositions and SHS synthesis steps were not exactly given in the study. In the studies by Kazhikenova *et al.* [13] and by Zharmenov *et al.* [14, 15], the theoretical principles behind the SHS of refractory materials (magnesia, chromite-magnesia, forsterite, dolomite and chamotte refractories) were studied. Only theoretical calculations were reported and pure aluminosilicate refractories were not considered in these studies. A recently published study by Mansurov *et al.* [16] reported the influence of mechanochemical treatment of CaO-SiO_2-Al_2O_3 system minerals used as components in a mixture for SHS synthesis of ceramics. But pure aluminosilicate ceramics were not considered in this study either. There are also few studies presented by Balmori-Ramirez *et al.* [17], Erharghawi *et al.* [18], Khabas *et al.* [19] and Anggono *et al.* [20] where the aluminium powder was successfully utilized as the raw material for mullite powder synthesis, but the possibilities of SHS utilization were not studied.

In the current work, the possibilities for energy savings in pure aluminosilicate ceramic synthesis and sintering by utilizing SHS were studied. Kaolinite and exothermically reactive aluminium powder were used as raw materials. The aim of the study was to synthesize low-energy-intensity pure aluminosilicate-based ceramic bodies by means of SHS in air atmosphere, which has not been previously reported. Air atmosphere enables a more economical and sustainable option for synthesis atmosphere compared to using pure oxygen. Thermodynamic calculations for the possible reactions and reaction paths were performed beyond earlier publications in this field to show the theoretical possibilities for SHS utilization in pure aluminosilicate ceramics processing. The thermal reactions, thermal expansion and formed phase- and microstructures after SHS were evaluated and compared to conventional reaction sintering of mullite. The effects of kaolinite powder heat-treatment and aluminium particle size on chemical reactions that were not previously reported with these raw material mixtures were also studied.

II. Experimental Procedure

(1) Starting materials

Commercially available kaolinite powder ($Al_2O_3 \cdot 2SiO_2 \cdot 2H_2O$ or $Al_2Si_2O_5(OH)_4$), aluminium oxide hydroxide (AlO(OH, boehmite) powder and aluminium (Al) powder were used as raw materials. Kaolinite was provided by Merck (average grain size < 6.68 μm, high kaolin purity), aluminium oxide hydroxide by Sasol Germany GmbH (average grain size < 0.77 μm) and aluminium powder by ECKA Granules (average grain sizes < 27 μm and the same air classified to 17 μm, purity 99 %). Four mixtures were prepared from the selected raw materials. Recipes were calculated for stoichiometric 3:2 mullite synthesis; details are presented in Table 1. The endothermic dehydration reaction in kaolinite was assumed to consume the exothermic heat of the SHS reaction. In order to study this effect, in Mixture 2 kaolinite powder was first heat-treated at 850 °C for 30 min in order to decompose the aluminosilicate hydrate, kaolinite, to metakaolin ($Al_2Si_2O_5$). Raw materials were mixed by means of high-energy attrition milling for 10 min in argon atmosphere. A short milling time was chosen in order to avoid any reactions during milling.

Table 1: Test matrix for mullite synthesis experiments.

Mixture no	Raw material 1	wt%	Raw material 2	wt%
1	Kaolinite powder	51.8	Aluminium oxide hydroxide	48.2
2	Heat-treated kaolinite powder	67.3	Al powder (27 μm)	32.7
3	Kaolinite powder	70.5	Al powder (27 μm)	29.5
4	Kaolinite powder	70.5	Al powder (17 μm)	29.5

(2) Compaction and sintering

For mullite reaction sintering experiments, attrition-milled mixtures were uniaxially cold pressed to pellets of the size 20*3 mm using approximately 25 MPa pressure. The pellets were then reaction-sintered in an ENTECH air chamber furnace. Sintering was performed in air atmosphere and in ambient air pressure with a heating rate of 3.3 °C/min up to 1600 °C. which was maintained for 1 h before cooling to room temperature with cooling rate of 5 °C/min.

For the SHS experiments, aluminium-containing attrition-milled mixtures were packed in a steel mould with diameter of 70 mm and with powder bed thickness of 25 mm. The packing pressure of the powder mixtures was about 26 MPa. The steel mould was coated with 2 mm graphite foil in order to reduce heat losses and facilitate mould release. A thermocouple was inserted into the powder bed to a depth of about 3 mm from the upper surface to measure the temperature during the process, and to indicate the reaction front propagation. The powder bed with the mould was preheated at 500 °C in a separate furnace in air atmosphere. The mould was then quickly transferred from the furnace and the preheated packed powder bed surface was then ignited in air atmosphere from the top surface using resistance heating.

(3) Characterization techniques

The thermal behaviour and reaction paths of raw materials and attrition-milled powder mixtures were studied using thermogravimetric analysis (TGA, Netzsch STA 449 F1 Jupiter) giving a simultaneous Differential Scanning Calorimetry signal (DSC). Tests were conducted in air atmosphere with a temperature range from 40 °C to 1400 °C with the heating rate of 10 °C/min. A qualitative mass spectrometer (QMS, Netzsch QMS 403 D Aëolos) coupled directly to the TGA device exhaust was used for evolved gas analysis. The thermal expansion of uniaxially pressed (5 kN) pellets with a diameter of 11.62 mm was measured in air atmosphere with temperature range of 20 °C to 1550 °C using a horizontal pushrod dilatometer (Adamel Lhomargy DI-24). Qualitative phase analyses were performed for raw materials and final products by using an X-ray diffractometer (XRD, Empyrean, PANalytical B.V., ALMELO, Netherlands) with CuKα radiation source, and analysed using HighScore Plus software. Microstructures of the final sintered bodies were observed using a scanning electron microscope (SEM, Jeol JSM 6360LV) equipped with electron-dispersive spectroscopy (EDS). SEM investigations were conducted on polished cross-sections coated with gold. Thermodynamic calculations for the possible reactions, reaction enthalpies and adiabatic temperatures were performed using FactSage thermochemical software with FToxid database.

III. Results and Discussion

(1) Characterization of starting materials

(a) *Phase composition*

XRD patterns of untreated kaolinite powder and kaolinite powder after heat-treatment at 850 °C for 30 min are presented in Fig. 1. XRD patterns reveal that untreated kaolinite powder mainly consists of kaolinite $Al_2O_3{\cdot}2SiO_2{\cdot}2H_2O$ phase, alternatively presented as $Al_2Si_2O_5(OH)_4$. The kaolinite powder heat-treated at 850 °C for 30 min. mainly showed aluminium silicate $Al_2O_3{\cdot}SiO_2$ (Al_2SiO_5) phase forming from kaolinite caused by dehydration, i.e. water release.

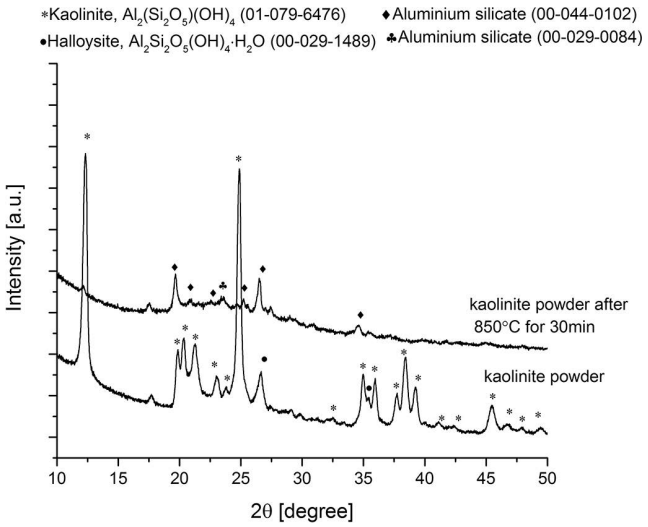

Fig. 1: XRD patterns of kaolinite and heat-treated kaolinite powders.

(b) *Thermal behaviour*

Fig. 2 shows the TGA/DSC/QMS-curve of kaolinite powder. An endothermic peak relating to the dehydration of the kaolinite into metakaolin phase can be seen at 510 °C (T_1). This includes water release according to following reaction, Eq. (1), presented by Yung-Feng *et al.* [9]:

$$Al_2O_3 \cdot 2SiO_2 \cdot 2H_2O \rightarrow Al_2O_3 \cdot 2SiO_2 + 2H_2O \quad (1)$$

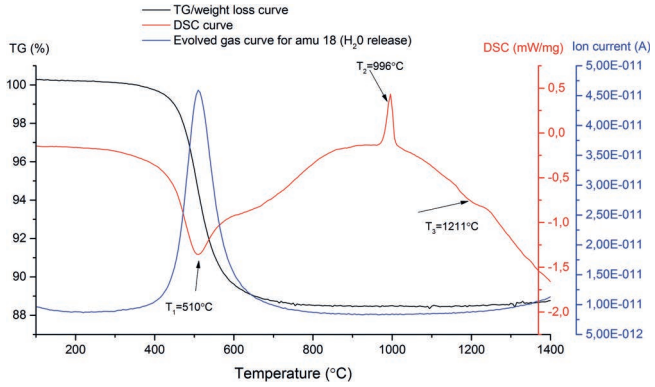

Fig. 2: Thermal behaviour of kaolinite powder.

At 996 °C (T_2), an exothermic peak related to the reorganization of the metakaolin into the Al-Si-spinel phase, $Si_3Al_4O_{12}$, and amorphous silica (SiO_2) phase, can be seen according to reaction Eq. (2) presented by Yung-Feng *et al.* [9]:

$$2(Al_2O_3 \cdot 2SiO_2) \rightarrow Si_3Al_4O_{12} + SiO_2 \quad (2)$$

At 1211 °C (T_3), mullite formation is starting according to the reaction in Eq. (3) presented by Yung-Feng *et al.* [9], resulting in mullite $3Al_2O_3{\cdot}2SiO_2$ and amorphous silica phases:

$$3Si_3Al_4O_{12} \rightarrow 2(3Al_2O_3 \cdot 2SiO_2) + 5SiO_2 \quad (3)$$

Because of the higher silica content in kaolinite than in mullite, an addition of alumina is needed to synthesize stoichiometric mullite. Eq. (4) presents a balanced reaction with a stoichiometric amount of alumina:

$$Si_3Al_4O_{12} + 5SiO_2 + 10Al_2O_3 \rightarrow 4(3Al_2O_3 \cdot 2SiO_2) \quad (4)$$

Fig. 3 shows the TGA/DSC-curve of aluminium powder ($d_{50} = 27\,\mu m$). Solid-state aluminium oxidation can be seen starting after 560 °C according to Eq. (5) and increase in weight:

$$4Al + 3O_2(g) \rightarrow 2Al_2O_3 \quad (5)$$

This is followed by aluminium melting at 660 °C. An exothermic peak is seen again at 996 °C, which could be attributed to accelerated liquid-state aluminium oxidation. The weight gain revealed that aluminium oxidation continues at high temperatures from 660 °C up to upper temperature limit of 1400 °C. After the accelerated oxidation after 1000 °C, oxidation continues with increasing rate as a function of the temperature. Trunov *et al.* [21] showed that, in aluminium powder oxidation, four distinct stages could be observed in the temperature range from 300 °C to 1500 °C. At the first stage, at temperatures below about 550 °C there was slow oxidation. At

about 550 °C, a transformation of amorphous alumina into γ-Al_2O_3 occurred, when the oxide layer thickness exceeded the critical thickness of amorphous alumina. The density of the γ - Al_2O_3 was greater than that of amorphous alumina, thus the γ-Al_2O_3 covered the aluminium surface only partially. At the second stage in the temperature range, about 550 – 660 °C, the oxidation rate increases rapidly until the γ-Al_2O_3 coverage becomes multilayered and continuous. At the third stage from about 650 °C to 1000 – 1100 °C, the oxidation rate continuously increased, related to the growth of a continuous γ-Al_2O_3 layer and its partial transformations into the structurally similar θ - Al_2O_3 polymorph. Finally, at the fourth oxidation stage above 1100 °C, there was also increase of the oxidation rate, related to the formation and growth of the α-Al_2O_3 oxide. All these four stages can be identified in Fig. 3.

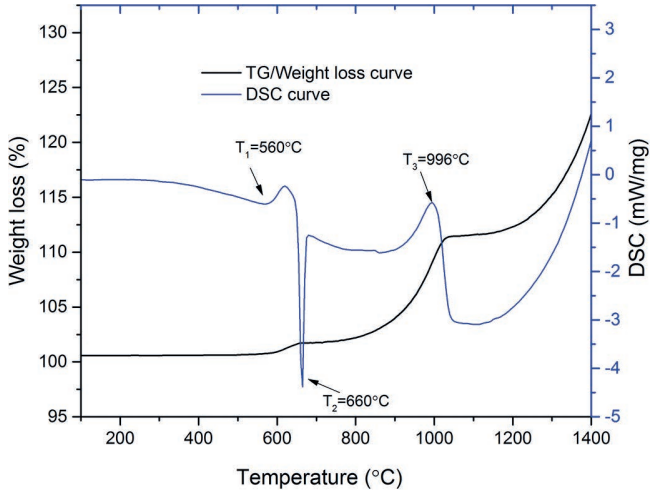

Fig. 3: Thermal behaviour of aluminium powder.

(2) Characterization of milled mixtures

(a) *Thermal behaviour, phase structure evolution*

Fig. 4 shows DSC-curves of the milled Mixtures 1 – 4. For Mixture 1, which does not contain aluminium, the DSC results show a first endothermic peak at 498 °C (T_1). That peak could be the dehydration of the kaolinite into the metakaolin according to presented Eq. (1) and also dehydration of aluminium oxide hydroxide, AlO(OH), according to following reaction (6):

$$2AlO(OH) \rightarrow Al_2O_3 + H_2O \qquad (6)$$

Obviously, for Mixture 2 containing heat-treated kaolinite, the kaolinite hydration reaction at 498 °C is missing. For Mixtures 3 and 4, the dehydration of the kaolinite into the metakaolin is observed at 498 °C according to Eq. (1). A different shape of the endothermic peak compared to Mixture 1 can be seen, because aluminium oxide hydroxide dehydration is missing. Aluminium-containing Mixtures 2 – 4 show exothermic solid-state aluminium oxidation starting at about 580 °C (T_2) according to Eq. (5) and endothermic aluminium melting at 660 °C (T_3). Exothermic peaks are seen again at 953 °C (T_4) which could be attributed to liquid-state aluminium oxidation. DSC results suggest that with the decrease in the aluminium particle size (difference between Mixture 3 and 4) aluminium oxidation accelerates, which seems obvious because of higher surface area. For all Mixtures 1 – 4, exothermic peaks observed at 993 °C (T_5) are probably caused by the reorganization of the metakaolin into the Al-Si-spinel phase according to Eq. (3). For aluminium-containing Mixtures 2 – 4, an exothermic peak is observed again at 1219 °C (T_6). For Mixture 2, which contains heat-treated kaolinite, the DSC signal stabilizes after the 1219 °C peak. Contrary to untreated kaolinite-containing Mixtures 3 and 4, it seems that the reaction is not finished within the measured temperature range. Contrary to the initial assumption, the dehydration of kaolinite does not significantly affect the heat balance of the reactions, as it occurs before, i.e. at lower temperature than other (exothermic) reactions. Thus, the kaolinite dehydration reaction occurring *in situ* in Mixtures 3 and 4 may even enhance the reactivity of the formed metakaolin phase.

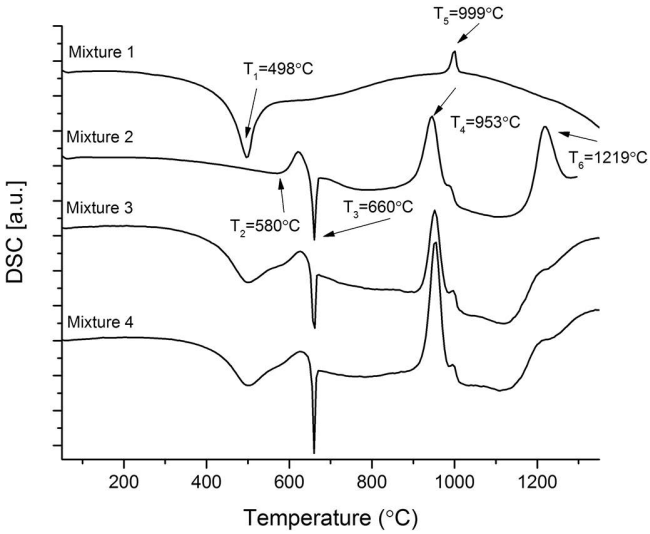

Fig. 4: DSC results of milled mixtures, presented in Table 1.

Fig. 5 shows TG-curves for the milled Mixtures 1 – 4. Mixture 1 and aluminium-containing Mixtures 3 and 4 show weight loss at about 498 °C (T_1) related to the dehydration reaction observed in the DSC curves. For Mixture 2 that contained heat-treated kaolinite this reaction is missing in the DSC curve and there is no weight loss observed for that mixture at that temperature. For aluminium-containing mixtures, aluminium oxidation starting approximately at 600 °C is seen as an increase in the weight loss curve. Another increase in the weight loss curve is observed after 900 °C and after 1200 °C relating to aluminium oxidation. TG-curves support the observation in DSC curves that with finer aluminium particle size (Mixture 4) the oxidation rate is quicker compared to Mixture 3. DSC results suggest that for heat-treated kaolinite oxidation stabilizes after 1219 °C. According to the TG-curves, the oxidation degree seems to be a little higher for heat-treated kaolinite powder in the temperature range from 600 °C to 1000 °C. After 1000 °C, oxidation seems to be higher for Mixtures 3 and 4 than for Mixture 2.

In their study [11], Esharghawi *et al.* have shown DTA curves for a mixture containing calcined kaolinite (heat-treated at 650 °C for 1 hour) and aluminium powder (average grain size < 45 μm). In our study, the DSC results

in Fig. 4 are similar to their results related to aluminium oxidation around 600 °C, aluminium melting at 660 °C and above 900 °C observed two exothermic peaks related to aluminium oxidation and the reorganization of the metakaolin. In contrast to their results, in our study, DSC results also reveal an exothermic peak at 1219 °C for Mixtures 2 – 4. This observed difference could be related to the use of finer aluminium in our study (average grain size < 27 μm and < 17 μm) which promotes aluminium oxidation.

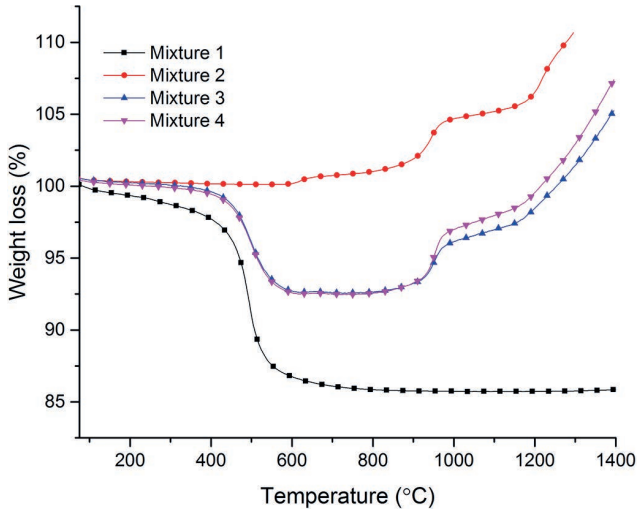

Fig. 5: TG-curves of the milled mixtures, presented in Table 1.

(a) *Thermal expansion characteristics*

The thermal expansion behaviour of the compressed material from Mixtures 1 – 4 is presented in Fig. 6. Mixture 1, where aluminium oxide hydroxide AlO(OH) was used as the source of aluminium instead of metallic Al, clearly shows shrinkage that accelerates when the temperature reaches 1000 °C. The first unique shrinkage step for this mixture visible at 500 °C can be attributed to the dehydration of kaolinite into metakaolin, but more importantly to the dehydration of AlO(OH). Significant sintering of the aluminosilicate powder at 1000 – 1200 °C is quite evident, followed by a step above 1250 °C most likely caused by a combination of mullite formation and phase transformation of aluminium oxide into the α-phase.

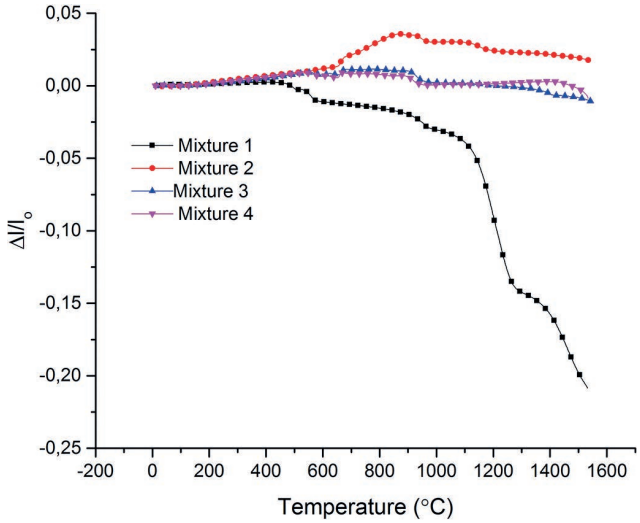

Fig. 6: Dilatometric curves of milled mixtures, presented in Table 1.

For mixtures containing metallic Al, despite showing very little length variation overall, some of the events described in the TG-curves and DCS results above are discernible in dilatometric curves as well. Mixtures 3 and 4 show a small dip above 540 °C followed by a sudden rise at 650 – 675 °C, the latter of which is also present for Mixture 2 and is probably caused by melting of the aluminium. Since Mixture 2 does not show clear events at 540 – 600 °C, it is safe to assume that the previously mentioned dip starting at 540 °C for Mixtures 3 and 4 is due to kaolinite dehydration. Other minute variations between the behaviour of Mixtures 2, 3 and 4 above 1000 °C are inconclusive.

All of the mixtures showed a minor shrinkage event below 1000 °C, most likely caused by reorganization of metakaolin into spinel phase. The large differences in the dimensional change between mixtures that either do or do not contain metallic Al, suggests that there is either a very large difference in compressibility of these powders, or that the powders containing Al do not densify in high temperatures and thus exhibit no sintering shrinkage associated with more conventional ceramic powder mixtures.

(3) Phase and microstructure analysis of the sintered bodies

(a) *Phase structure analysis of reaction-sintered specimens*

Phase structure analysis of the final products after reaction sintering of Mixtures 1 – 4 is presented in Fig. 7. It was observed that after reaction sintering there were differences in the specimen's phase structure homogeneity between different mixtures. Reaction sintering of Mixture 1 and 2 resulted in uniform phase structure, but for Mixtures 3 and 4, there was a difference between the interior and the surface phase structure. XRD patterns for test Mixtures 1 and 2 showed stoichiometric mullite as major phase and minor aluminium oxide phase. XRD patterns for test Mixtures 3 and 4 showed aluminium oxide in both the surfaces. For these mixtures, the specimen's interiors showed metallic silicon and aluminium phases in addition to aluminium oxide. These results suggest that mullite formation is possible by reaction sintering by using heat-treated kaolinite and aluminium powder as raw materials. When using untreated kaolinite and aluminium as starting material, only very minor mullite peaks are detected and the resulting final phase structure is aluminium oxide after reaction sintering at 1600 °C for 1 h. It should be noted that amorphous SiO_2 detection from XRD curves is challenging so probably the final phase structure in Mixtures 3 and 4 also contains amorphous SiO_2. It could be the assumed that also in Mixtures 3 and 4 aluminium oxide and silicon oxide will eventually react to form mullite, only if it is kinetically possible. Additionally, after reaction sintering kaolinite and aluminium mixtures, the formed specimen's phase structure is not homogenous and its interior showed metallic silicon and residual aluminium phases.

(b) *Phase structure analysis of SHS specimens*

Preheated packed powder bed surfaces of Mixtures 2 – 4 were ignited in air atmosphere from the top surface using

resistance heating. The exothermic reaction detected in the DSC results (in Fig. 4) at above 900 °C related to aluminium oxidation seems to ignite the SHS reaction for all aluminium-containing Mixtures 2 – 4. After initialization the reaction proceeded in self-sustaining manner through the entire test specimens from the top surface to the bottom. The highest measured temperature of the specimens during the SHS reaction was 1675 °C according to the thermocouple. Thus, in comparison to an earlier publication of Esharghawi *et al.* [11] where the SHS experiments were performed in flowing oxygen, our experiment proves that the SHS also succeeded in air atmosphere using similar raw materials mixtures. An air atmosphere is a more economic and sustainable option for synthesis compared to using pure oxygen.

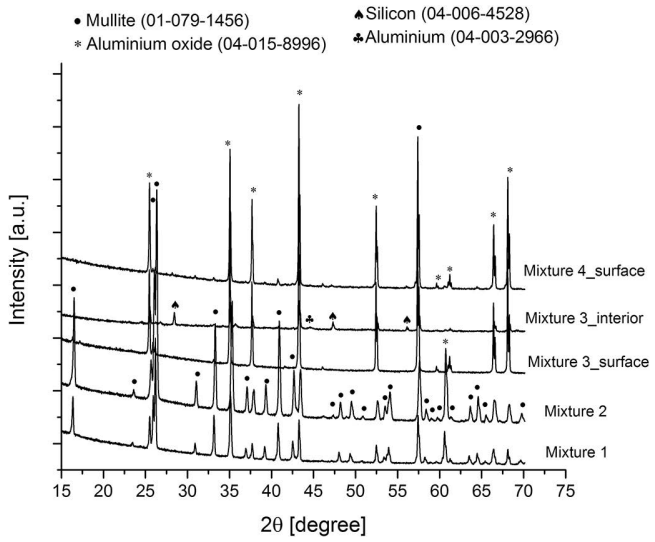

Fig. 7: XRD curves for reaction sintered mixtures, presented in Table 1.

Fig. 8 shows the XRD patterns of final test pieces after SHS. For all test Mixtures 2 – 4, the resulting phase structure after SHS was aluminium oxide and metallic silicon. Also small metallic aluminium peaks were seen for kaolinite-powder-containing Mixtures 3 and 4. The difference between the aluminium particle size in Mixtures 3 and 4 was attributed to the amount of metallic aluminium: with finer aluminium particle size the metallic aluminium peak intensities were smaller. It could therefore be suggested that with finer aluminium particle size the aluminium oxidation is more effective, and less metallic aluminium is left unreacted. For heat-treated kaolinite containing test Mixture 2, it seems that metallic aluminium has reacted with metallic silicon, because aluminium silicon peaks are visible in the XRD pattern.

Esharghawi *et al.* [11] have reported in their study the significant phases as being mullite, quartz, α-alumina and silicon metal with traces of aluminium metal after SHS experiments in flowing oxygen. Thus, flowing oxygen and air atmosphere seem to result in different phase structures after SHS, because mullite and quartz peaks are not visible after SHS in air. This could result from there being more oxygen available for the reaction to be completed.

Comparison to other previous publications in this field is not unequivocal because similar raw material combinations do not exist in other publications. Podbolotov *et al.* [12] have reported a mullite phase structure together with potassium aluminosilicate, corundum and microcline when 85 % kaolin and 15 % aluminium were used as raw materials together with potassium water glass (potassium metasilicate) as binder and different additives such as boric acid and sodium silicon fluoride.

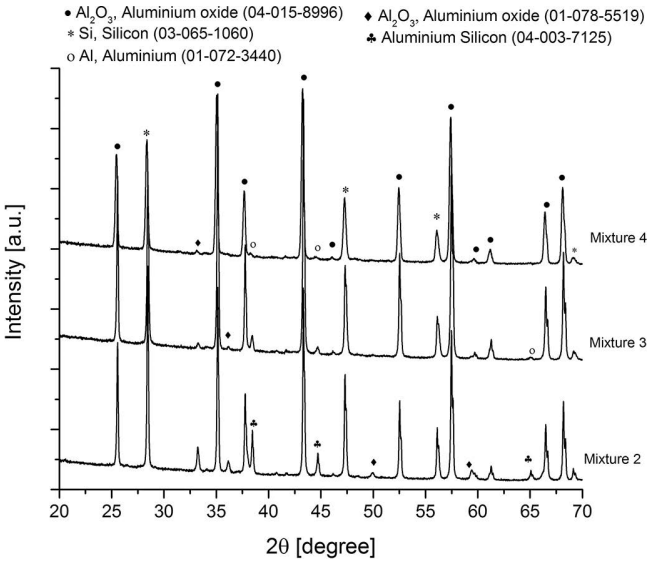

Fig. 8: XRD patterns after SHS for milled mixtures, presented in Table 1.

In order to confirm the reactions leading to the formation of mullite, SHS test pieces were post-treated at 1600 °C for 1 h. The XRD results after that post-treatment are shown in Fig. 9. After this post-treatment, all pieces corresponding to the test Mixtures 2 – 4 resulted in a mullite and aluminium oxide phase structure.

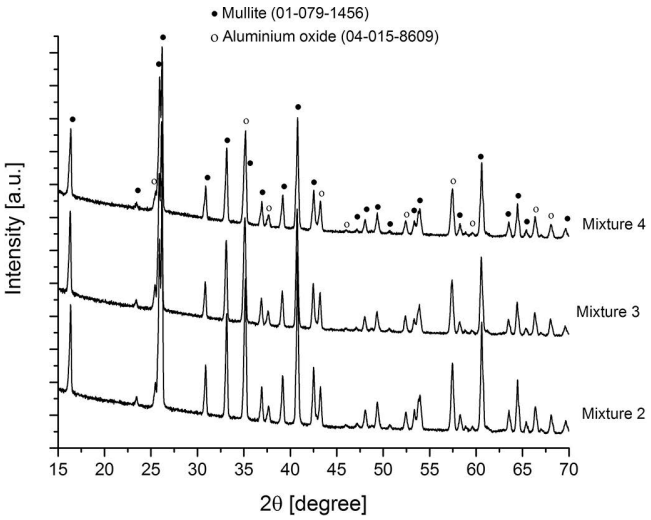

Fig. 9: XRD patterns of post-treated SHS pieces.

The difference between tthe reaction sintering and SHS results indicate that it is possible to affect the reaction path by employing SHS. Fast ignition of the reactions results in different phases than with slow heating. Bigger specimen sizes in the SHS test results in lower heat losses which make the SHS reaction possible but also change the reactions and the end result.

(c) ***Microstructural analysis of reaction-sintered specimens***

The SEM micrographs in Fig. 10 (a-d) show the microstructure cross-sections after reaction sintering experiments for (a) Mixture 1 of kaolinite and aluminium oxide hydroxide (b) Mixture 2 of heat-treated kaolinite and aluminium (27 µm) (c) Mixture 3 of kaolinite and aluminium (27 µm) and (d) Mixture 4 of kaolinite and aluminium (17 µm). The micrographs reveal much higher porosity in the aluminium-containing Mixtures 2, 3, and 4 than in Mixture 1 containing aluminium oxide hydroxide as the aluminium source. These micrographs support the differences in sinterability between these mixtures as detected in the dilatometer curves. For Mixture 1 the dilatometer curve showed first densification and then the reactions. For the aluminium-containing mixtures, the reactions dominated and the densification phase was absent, resulting in a more porous microstructure.

(d) ***Microstructural analysis of SHS specimens***

Fig. 11 (a-b) shows the SEM micrographs of aluminium (d_{50} =27 µm)-containing mixtures with (a) heat-treated (Mixture 2) and (b) untreated (Mixture 3) kaolinite after SHS. The microstructures seemed to be quite similar and a high fraction of porosity was observed. Two different phase areas were seen: denser areas of few tens of micrometres and finer particles with porosity. According to EDS analysis the denser areas are silicon rich and the finer particles are, on the contrary, aluminium oxide rich areas.

(4) Thermodynamic calculations

Thermodynamic calculations for the possible reactions and reaction paths were performed beyond earlier publications in this field to show the theoretical possibilities for SHS utilization in pure aluminosilicate ceramics processing. Thermodynamic calculations for the possible reactions, reaction enthalpies and adiabatic temperatures were performed using FactSage thermochemical software with FToxid database.

(a) ***Reaction sintering experiments***

Reaction sintering of the powder Mixture 1 of kaolinite and aluminium oxide hydroxide, resulted in mullite phase structure formation, thus the following reactions were assumed:

After 495 °C: $$Al_2O_3 \cdot 2SiO_2 \cdot 2H_2O \rightarrow Al_2O_3 \cdot 2SiO_2 + 2H_2O \quad (1)$$

$$2AlO(OH) \rightarrow Al_2O_3 + H_2O \quad (6)$$

After 999 °C: $$2(Al_2O_3 \cdot 2SiO_2) \rightarrow Si_3Al_4O_{12} + SiO_2 \quad (2)$$

After 1211 °C: $$3Si_3Al_4O_{12} \rightarrow 2(3Al_2O_3 \cdot 2SiO_2) + 5SiO_2 \quad (3)$$

Aluminium oxide resulting in Eq. (6) could react with silicon oxide resulting from Eq. (2) forming a mullite phase structure according to Eq. (7):

$$3Al_2O_3 + 2SiO_2 \rightarrow (3Al_2O_3 \cdot 2SiO_2) \quad (7)$$

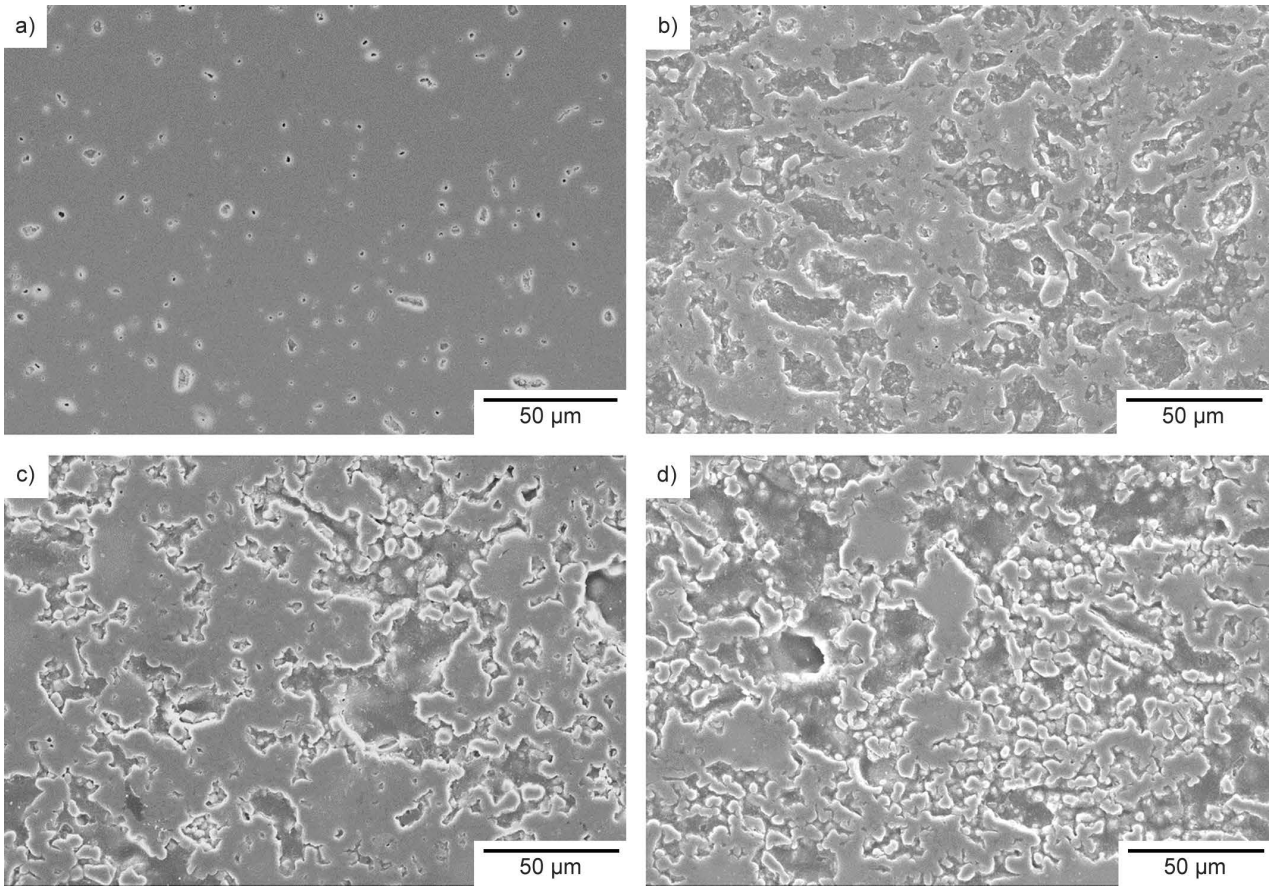

Fig. 10: SEM images of cross-sections of reaction-sintered specimens: (a) Mixture 1 (b) Mixture 2 (c) Mixture 3 and (d) Mixture 4 with 500x magnification.

Thus, the following total reaction was assumed to take place during reaction sintering of powder Mixture 1 of kaolin and aluminium oxide hydroxide:

$$Al_2O_3 \cdot 2SiO_2 \cdot 2H_2O + 4AlO(OH) \rightarrow 3Al_2O_3 \cdot 2SiO_2 + 4H_2O \quad (8)$$

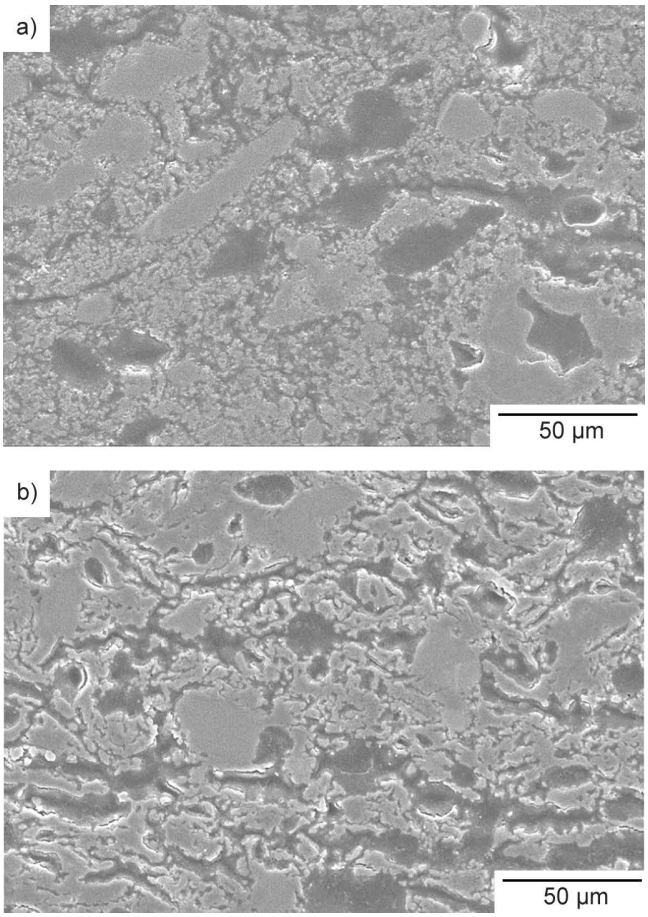

Fig. 11: SEM images of cross-sections after SHS for (a) Mixture 2 and (b) Mixture 3 with 500x magnification.

Table 2 summarizes the calculated reaction enthalpies for presented reactions for Mixture 1. The conclusion from this is that the mullite formation of the kaolinite and aluminium oxide hydroxide mixture is endothermic in nature and thus external heat is required. For the reactions (2) and (3), thermodynamic data was not available in the database used.

Table 2: Calculated reaction enthalpies for assumed reactions during reaction sintering of Mixture 1.

Reaction	Reaction enthalpy, ΔH [kJ]
(1)	+191
(6)	+ 25
(7)	+29
(8)	+115

In order to the define the reaction routes for aluminium-containing mixtures, all the Mixtures 1 – 4 were heat-treated at 1100 and 1300 °C. Fig. 12 (a-d) shows XRD curves after 1100 °C, 1300 °C and 1600 °C for (a) Mixture 1, (b) Mixture 2, (c) Mixture 3 and (d) Mixture 4. Mixture 1 showed aluminium silicate and aluminium oxide phase at 1100 °C, and at 1300 °C mullite phase in addition to aluminium oxide phase, which supported the above-suggested reaction paths for Mixture 1.

According to Fig. 12 XRD, patterns at 1100 °C for Mixture 2, which contain heat-treated kaolinite and aluminium, showed aluminium oxide phase structure containing also metallic silicon and aluminium phases. This observation suggests that aluminium reduces SiO_2 to metallic silicon according to Eq. (9):

$$4Al + 3SiO_2 \rightarrow 3Si + 2Al_2O_3 \quad (9)$$

Perhaps it could also be possible that aluminium reduces SiO_2 from metakaolin as well, according to Eq. (10):

$$Al_2O_3 \cdot 2SiO_2 + 2Al \rightarrow 2Si + 2Al_2O_3 \quad (10)$$

According to Fig. 12, at 1300 °C the XRD pattern for Mixture 2 already showed mullite peaks in addition to aluminium oxide phase. There were still metallic silicon peaks, but the metallic aluminium peaks had disappeared, so it could be concluded that the aluminium was fully oxidized. At 1600 °C the metallic silicon peaks disappeared and the phase structure consisted of mullite and aluminium oxide phases. Thus, after 1300 °C it was assumed that metallic silicon can further oxidize to silicon oxide according to (11):

$$Si + O_2(g) = SiO_2 \quad (11)$$

The formed silicon oxide can then react with aluminium oxide in the structure to finally form mullite according to Eq. (7):

$$3Al_2O_3 + 2SiO_2 \rightarrow (3Al_2O_3 \cdot 2SiO_2) \quad (7)$$

The total reaction route during the reaction sintering of Mixture 2 could be suggested to be the following:

After 953 °C: $4Al + 3O_2(g) \rightarrow 2Al_2O_3(s)$ (5)

After 996 °C: $2(Al_2O_3 \cdot 2SiO_2) \rightarrow Si_3Al_4O_{12} + SiO_2$ (2)

$4Al + 3SiO_2 \rightarrow 3Si + 2Al_2O_3$ (9)

After 1219 °C: $Si + O_2 \rightarrow SiO_2$ (11)

$3Si_3Al_4O_{12} \rightarrow 2(3Al_2O_3 \cdot 2SiO_2) + 5SiO_2$ (3)

$3Al_2O_3 + 2SiO_2 \rightarrow (3Al_2O_3 \cdot 2SiO_2)$ (7)

According to Fig. 12, at 1100 °C for Mixtures 3 and 4, which contain kaolinite, the XRD patterns show aluminium oxide phase structure involving also metallic silicon and aluminium. For these mixtures at 1300 °C metallic silicon and aluminium peaks were still visible in addition to aluminium oxide as a major phase. Unlike for metakaolin-containing Mixture 2, there were no mullite peaks at 1300 °C but the peaks of θ - Al_2O_3 appeared. At 1600 °C, all the metallic silicon and aluminium peaks disappeared and the major phase was aluminium oxide while very minor mullite peaks started to appear. The total reaction route during the reaction sintering of Mixture 3 and 4 could be suggested to be similar to that for Mixture 2, although in Mixtures 3 and 4 there was also kaolinite dehydration that occurs according to Equation (1) after 495 °C. But it could be detected that during the reac-

tion sintering mixture of kaolinite and aluminium, mullite formation seems to be much slower than is the case when metakaolin and aluminium are used. This could be due to the differences in reactivity between kaolinite and metakaolin. One possibility is that the kaolinite dehydration reaction occurring *in situ* may enhance the reactivity of the formed metakaolin phase and thus it could also be possible that aluminium reduces SiO_2 from metakaolin according to Equation (10) in Mixtures 3 and 4 too. It could also be assumed that in Mixtures 3 and 4 aluminium oxide and silicon oxide will eventually react to form mullite, provided that it is kinetically possible. Mechanical properties of metakaolin could be also different to those of kaolinite and because of that grinding and mixing during attrition milling could be more efficient in the case of the heat-treated kaolinite. It could be also possible that kaolinite dehydrates in the attritor mill to some extent, hindering the mixing process.

Table 3 summarizes the calculated reaction enthalpies and adiabatic temperatures for presented reactions for Mixtures 2 – 4. For the reactions (2) and (3), the thermodynamic data was not available in the database used. For Mixture 2, the endothermic dehydration reaction (1) was missing. The aluminium oxidation reaction (5), the aluminium-reducing silicon oxide to metallic silicon reaction (9) and the further oxidizing of silicon (11) are all exothermic reactions. The kaolinite dehydration (1) and mullite formation reactions (7) are only endothermic reactions requiring external energy. According to these thermodynamic calculations, the reaction energy balance for mullite formation from aluminium and kaolinite mixtures is highly exothermic in nature only if sufficient oxygen is available for the reactions to be completed.

Table 3: Calculated reaction enthalpies for assumed reactions during reaction sintering of Mixtures 2 – 4, presented in Table 1.

Reaction	Reaction enthalpy, ΔH [kJ]	T_{ad} [°C]
(1)	+191	-
(5)	-3351	9439
(9)	-619	1902
(11)	-960	-
(7)	+29	-

In the study by Podbolotov *et al.* [12], aluminium powder, quartz sand and kaolin were used as raw materials for mixtures. They have suggested similar chemical processes corresponding to our Eqs. (7), (9) and (11). In their study, the reaction enthalpies and adiabatic temperatures for the presented reactions were missing.

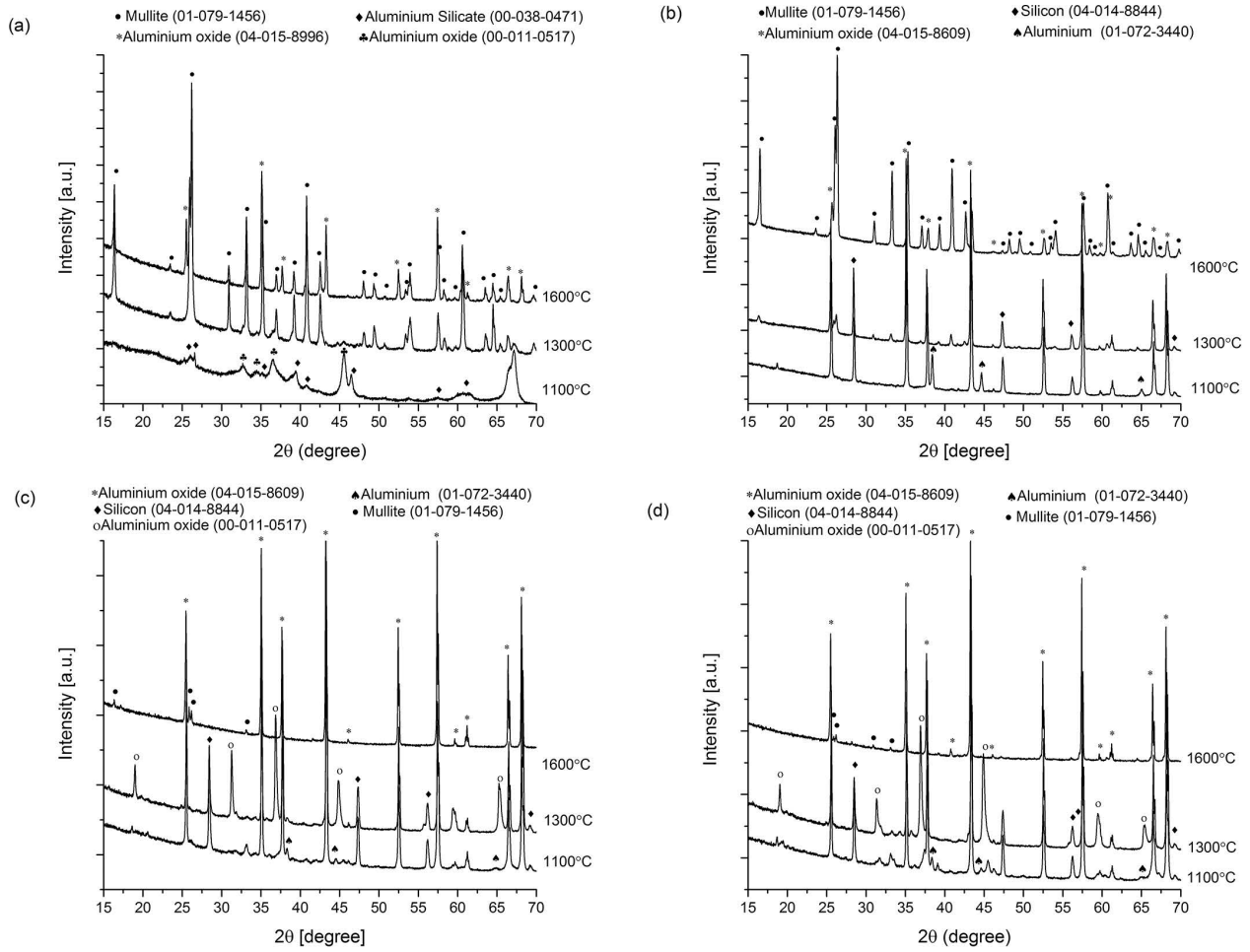

Fig. 12: XRD results after 1100 °C, 1300 °C and 1600 °C for (a) Mixture 1 (b) Mixture 2 (c) Mixture 3 and (d) Mixture 4.

(b) ***SHS experiments***

As the results in Table 3 show, the aluminium oxidation is a highly exothermic reaction only if sufficient oxygen is available for the reaction. In addition, the aluminium-reducing silicon oxide to metallic silicon reaction is exothermic as is the further oxidizing of silicon. The kaolinite dehydration and mullite formation reactions are only endothermic, requiring external energy. The dehydration of kaolinite does not significantly affect the heat balance of the reactions as it occurs before, i.e. at a lower temperature than other (exothermic) reactions. The energy balance in the total reactions indicates the release of energy, thus in energy terms there is great potential for aluminosilicate-based ceramic synthesis when aluminium is used as a raw material. Theoretically, the saving in heating energy could be as high as 70 % if the furnace temperature could be decreased from 1600 °C to 900 °C.

However, the resulting SHS materials from Mixtures 2–4 were inhomogeneous and porous, with inadequate mechanical properties. Reasons for this could relate to the inadequate densification mechanism related, for example, to the absence of clear liquid phase. In addition, the specimens were not densified by pressing after SHS. Future research is needed to enable the full utilization of SHS to obtain solid pieces with acceptable mechanical properties. One possibility is to add oxidizing raw materials to provide sufficient oxygen for the reactions to be completed.

After post-treatment of the SHS specimens, the XRD results show a mullite- and aluminium-oxide-containing phase structure. Thus, the following reactions are assumed to have taken place during the post-treatment:

$$Si + O_2 \rightarrow SiO_2 \quad (11)$$

$$3Al_2O_3 + 2SiO_2 \rightarrow (3Al_2O_3 \cdot 2SiO_2) \quad (7)$$

After SHS and post-treatment, all the aluminium-containing mixtures showed a mullite and aluminium oxide phase structure. After reaction sintering of kaolinite and aluminium, the mixtures showed mainly aluminium oxide phase structure. In addition, the formed phase structure was heterogeneous and the specimen's interior also showed metallic silicon and aluminium phases. Thus, it seems that mullite is formed quicker after SHS than in conventional reaction sintering if aluminium and untreated kaolinite are used as raw materials.

IV. Conclusions

In the current work, the possibilities were studied for saving energy in pure aluminosilicate-based ceramic synthesis and sintering based on the use of SHS in air atmosphere. Kaolinite powder, aluminium oxide hydroxide and exothermically reactive aluminium powder were used as raw materials. Four mixtures were prepared from the selected raw materials for the stoichiometric 3:2 mullite synthesis. The thermal reactions and formed phase- and microstructures were compared to the conventional reaction sintering of mullite. The role of the alumina source, the effect of kaolinite heat-treatment and aluminium particle size were studied. The endothermic dehydration reaction in kaolinite was assumed to consume the exothermic heat of the SHS reaction. To study this, in one mixture kaolinite powder was first heat-treated at 850 °C for 30 min in order to effect decomposition of the aluminosilicate hydrate, kaolinite, to metakaolin. All the mixtures were prepared by means of attrition milling in argon atmosphere.

Reaction sintering of the kaolinite and aluminium oxide hydroxide mixture resulted in mullite ceramic pieces. Reaction sintering of the heat-treated kaolinite, metakaolin, and aluminium powder also resulted in mullite ceramic pieces. But reaction sintering of the untreated kaolinite and aluminium powder mixture resulted in aluminium- and silicon oxide phase structures and only minor mullite phase was detected. Additionally, after reaction sintering of the kaolinite and aluminium mixture, the phase structures of the formed pieces were not homogeneous and their interiors showed metallic silicon and residual aluminium phases. This could result from the differences in reactivity between kaolinite and heat-treated kaolinite. One possibility is that the kaolinite dehydration reaction occurring *in situ* may enhance the reactivity of the formed metakaolin phase and thus it could be possible that aluminium reduces SiO_2 from metakaolin as well, which affects the reaction rate. Dilatometer results showed huge differences in the thermal expansion behaviour and sinterability between aluminium oxide hydroxide and aluminium powder as the alumina source. Aluminium oxide hydroxide clearly showed shrinkage and significant sintering, but the mixtures containing metallic Al showed very little variation in length overall. The large differences in dimensional change between mixtures that either do or do not contain metallic Al suggest that there is either a very large difference in the compressibility of these powders or that the powders containing Al do not densify in high temperatures and thus do not exhibit the sintering shrinkage associated with more conventional ceramic powder mixtures. It should be also noted that the particle size of the aluminium oxide hydroxide is much smaller than for aluminium, which promotes sinterability.

On the basis of the thermal behaviour analysis and thermodynamic calculations performed, it is apparent that mullite formation from kaolinite and aluminium oxide hydroxide as the alumina source is endothermic in nature, thus external energy is needed. When exothermically reactive raw material is used, i.e. aluminium powder, the DSC results reveal a highly exothermic reaction starting above 900 °C. This reaction, which is related to aluminium oxidation, ignited the SHS reaction and after initialization the reaction proceeded in a self-sustaining manner through entire test pieces in air atmosphere. The highest recorded temperature during SHS reaction was 1675 °C. According to thermodynamic calculations, in addition to the aluminium oxidation reaction, the aluminium-reducing silicon oxide to metallic silicon reaction and the further oxidization of silicon are exothermic. Thus, the total energy balance for mullite formation from aluminium and kaolinite mixtures is highly exothermic in nature only if sufficient oxygen is available for the reactions to be completed. SHS results in Al_2O_3 - Si phase structure formation in the test pieces. The difference between the reaction sintering and SHS results indicate that it is possible to affect the reaction path by employing SHS. Contrary to the first assumption, the dehydration of kaolinite does not signif-

icantly affect the heat balance of the reactions as it occurs before, i.e. at lower temperature than other (exothermic) reactions. Thus, this affects the total energy balance, but not the SHS reaction itself or reaction sintering. Fast ignition of the reactions results in different phases than with slow heating. Bigger specimen sizes in the SHS tests not only make the SHS reaction possible owing to lower heat losses but also changes the reactions and the end-result. Theoretically, the saving in heating energy could be as high as about 70 % if the furnace temperature could be reduced from 1600 °C to 900 °C. Thus, in energy terms, potential exists for utilizing SHS in aluminosilicate-based ceramic synthesis. However, the resulting SHS materials were inhomogeneous, porous and did not exhibit acceptable mechanical properties, so future research is needed to properly utilize SHS. One possibility is to add oxidizing raw materials in order to provide sufficient oxygen for the reactions to be completed.

Acknowledgements

The research was funded by the Academy of Finland, project CeraTail. The authors would like to thank Mr Mika Heikkinen for his part in the experimental work.

References

1 Kang, T.S., Park, C-H., Kim, S.H.: Characteristics of exothermic reaction fronts in the gasless combustion system, *Ceram. Int.,* **37**, 825 – 833, (2011).

2 Merzhanov, A.G.: History and recent developments in SHS, *Ceram. Int.*, **21**, [5], 371 – 379, (1995).

3 Cao, G., Orrù, R.: Self-propagating reactions for environmental protection: State of the art and future directions, *Chem. Eng. J.,* **87**, [2], 239 – 249, (2002).

4 Mossino, P.: Review some aspects in self-propagating high-temperature synthesis, *Ceram. Int.*, **30**, 311 – 332, (2004).

5 Dong, Y., Feng, X., Feng, X., Ding, Y., Liu, X., Meng, G.: Preparation of low-cost mullite ceramics from natural bauxite and industrial waste fly ash, *J. Alloy. Compd.*, **460**, 599 – 606, (2008).

6 Zaki, Z.I., Ewais, E.M.M., Rashad, M.M.: Review novel route for combustion synthesis of zirconia-mullite/TiB_2 composites, *J. Alloy. Compd.*, **467**, 288 – 292, (2009).

7 Chen, C.Y., Lan, G.S., Tuan, W.H.: Preparation of mullite by the reaction sintering of kaolinite and alumina, *J. Eur. Ceram. Soc.*, **20**, 2519 – 2525, (2000).

8 Zaki, Z.I.: Combustion synthesis of mullite-titanium boride composite, *Ceram. Int.*, **35**, 673 – 678, (2009).

9 Chen, Y-F., Wang, M-C., Hon, M-H.: Phase transformation and growth of mullite in kaolin ceramics, *J. Eur. Ceram. Soc.*, **24**, 2389 – 2397, (2004).

10 Yeh, C.L., Kao, W.C.: Preparation of TaB/TaB_2/mullite composites by combustion synthesis involving aluminothermic reduction of oxide precursors, *J. Alloy. Compd.*, **615**, 734 – 739, (2014).

11 Esharghawi, A., Penot, C., Nardou, F.: Elaboration of porous mullite-based materials via SHS reaction, *Ceram. Int.*, **36**, [1], 231 – 239, (2010).

12 Podbolotov, K.B., Dyatlova, E.M., Popov, R. Yu.: Ceramic refractory SHS-coatings based on the system, Al-SiO_2, *Refract. Ind. Ceram.,* **54**, [5], 31 – 36, (2014).

13 Kazhikenova, S. Sh., Nurkenov, O.A., Satbaev, B.N.: Theoretical aspects of the creation of highly efficient refractories on the basis of SHS technology, *Refract. Ind. Ceram.,* **52**, [1], 55 – 60, (2011).

14 Zharmenov, A.A., Satbaev, B.N., Kazhikenova, S. Sh., Nurkenov, O.A.: Development of refractory materials prepared by SHS technology, *Refract. Ind. Ceram.* **52**, [4], 40 – 48, (2011).

15 Zharmenov, A.A., Satbaev, B.N., Kazhikenova, S. Sh., Nurkenov O.A.: Development of new refractory material by SHS-technology based on kazakhstan republic raw material resources, *Refract. Ind. Ceram.*, **53**, [3], 47 – 54, (2012).

16 Mansurov Z.A., Mofa N.N., Sadykov B.S., Sabaev Zh. Zh., Bakkara A.E: Mechanochemical treatment, structural peculiarities, properties, and reactivity of SHS systems based on natural materials. 4. Production of SHS ceramics based on mechonoactivated materials, *J. Eng. Phys. Thermophys.*, **89**, [1], 230 – 237, (2016).

17 Balmori-Ramirez, H.: Dense mullite from attrition-milled kyanite and aluminum metal, *J. Am. Ceram. Soc.,* **87**, [1], 144 – 146, (2004).

18 Esharghawi, A., Penot, C., Nardou, F.: Contribution to porous mullite synthesis from clays by adding al and mg powders, *J. Eur. Ceram. Soc.,* **29**, [1], 31 – 38, (2009).

19 Khabas, A., Nevvonen, O.V., Vereshchagin, V.I.: Synthesis of mullite in the presence of nanodisperse aluminium powder, *Refract. Ind. Ceram.*, **46**, [1], 71 – 75, (2005).

20 Anggono, J., Derby, B.: Mullite formation from the pyrolysis of aluminium-loaded polymethylsiloxanes: the influence of aluminium powder characteristics, *J. Eur. Ceram. Soc.*, **26**, [7], 1107 – 1119, (2006).

21 Trunov, M.A., Schoenitz, M., Zhu, X., Dreizin, E.L.: Effect of polymorphic phase transformations in Al_2O_3 film on oxidation kinetics of aluminum powders, *Combust. Flame,* **140**, 310 – 318, (2005).